Dynamics transitions at the outer vestibule of the KcsA potassium channel during gating

H. Raghuraman, Shahidul M. Islam, Soumi Mukherjee, Benoit Roux, and Eduardo Perozo[1]

Department of Biochemistry and Molecular Biology, Center for Integrative Sciences, The University of Chicago, Chicago, IL 60637

Edited by Richard W. Aldrich, The University of Texas at Austin, Austin, TX, and approved December 13, 2013 (received for review September 9, 2013)

In K^+ channels, the selectivity filter, pore helix, and outer vestibule play a crucial role in gating mechanisms. The outer vestibule is an important structurally extended region of KcsA in which toxins, blockers, and metal ions bind and modulate the gating behavior of K^+ channels. Despite its functional significance, the gating-related structural dynamics at the outer vestibule are not well understood. Under steady-state conditions, inactivating WT and noninactivating E71A KcsA stabilize the nonconductive and conductive filter conformations upon opening the activation gate. Site-directed fluorescence polarization of 7-nitrobenz-2-oxa-1,3-diazol-4-yl (NBD)-labeled outer vestibule residues shows that the outer vestibule of open/conductive conformation is highly dynamic compared with the motional restriction experienced by the outer vestibule during inactivation gating. A wavelength-selective fluorescence approach shows a change in hydration dynamics in inactivated and noninactivated conformations, and supports a possible role of restricted/bound water molecules in C-type inactivation gating. Using a unique restrained ensemble simulation method, along with distance measurements by EPR, we show that, on average, the outer vestibule undergoes a modest backbone conformational change during its transition to various functional states, although the structural dynamics of the outer vestibule are significantly altered during activation and inactivation gating. Taken together, our results support the role of a hydrogen bond network behind the selectivity filter, side-chain conformational dynamics, and water molecules in the gating mechanisms of K^+ channels.

ion channel | EPR spectroscopy | REES | pulsed EPR

The functional behavior of K^+ channels is defined by a series of structural rearrangements associated with the processes of activation and inactivation gating (1–6). In response to a prolonged stimulus and in the absence of an N-terminal inactivating particle, most K^+ channels become nonconductive through a process known as C-type inactivation (7). This C-type inactivation is crucial in controlling the firing patterns in excitable cells and is fundamental in determining the length and frequency of the cardiac action potential (8). C-type inactivation is inhibited by high extracellular K^+ (9, 10), and the blocker tetraethylammonium (TEA) (11) can also be slowed down in the presence of permeant ions with a long residence time in the selectivity filter (Rb^+, Cs^+, and NH^{4+}) (10).

The prokaryotic pH-gated K^+ channel KcsA shares most of the mechanistic properties of C-type inactivation in voltage-dependent K^+ channels (5, 6, 12–16). Recent crystal structures of open/inactivated KcsA reveal that there is a remarkable correlation between the degree of opening at the activation gate and the conformation and ion occupancy of the selectivity filter (5). In KcsA, the selectivity filter is stabilized by a hydrogen bond network, with key interactions between residues Glu71, Asp80, and Trp67 and a bound water molecule (17). Disrupting this hydrogen bond network favors the conductive conformation of the selectivity filter (12, 13, 15).

Early electrophysiological experiments have suggested that the outer vestibule (around T449 residue in *Shaker* and Y82 residue in KcsA) undergoes significant conformational rearrangement during C-type inactivation gating (16, 18, 19). However, comparison of the WT KcsA crystal structure, where the filter is in its conductive conformation, with either the structure obtained with low K^+ (collapsed filter) (17) or the crystal structure of open-inactivated KcsA with maximum opening (inactivated filter) (5) does not show major conformational changes in the outer vestibule that would explain these results (Fig. 1*A*). We have suggested that this apparent discrepancy can be understood if we take into consideration the potential differences in the dynamic behavior of the outer vestibule changes as the K^+ channel undergoes its gating cycle (16).

We have probed the gating-induced structural dynamics at the outer vestibule of KcsA using site-directed fluorescence and site-directed spin labeling and pulsed EPR approaches in combination with a recently developed computational method, restrained ensemble (RE) simulations. RE simulation was used to constrain the outer vestibule using experimentally derived distance histograms in different functional states (closed, open/inactivated, and open/conductive) and to monitor the extent of backbone conformational changes during gating. To this end, we took advantage of our ability to stabilize both the open/conductive (E71A mutant) and the open/inactivated (WT) conformations of KcsA upon opening the activation gate under steady-state conditions (Fig. 1*B*).

Our data show that the outer vestibule in the open/conductive conformation is highly dynamic. In addition, the red edge excitation shift (REES) points to a change in hydration dynamics between conductive and nonconductive outer vestibule conformations, suggesting a role of restricted water molecules in C-type inactivation gating. We suggest that, on average, the backbone conformation of the outer vestibule does not change significantly between different functional states but that local dynamics change significantly, underlining the importance of the hydrogen bond network behind the selectivity filter and the microscopic observables (e.g., dynamics of hydration) in K^+ channel gating and C-type inactivation.

Significance

C-type inactivation gating in K^+ channels plays an important role in controlling the firing patterns of excitable cells and is fundamental in determining the length and frequency of the cardiac action potential. At a molecular level, toxins, blockers, and metal ions bind to the outer vestibule and modulate the functional behavior of K^+ channels. Using KcsA, we show that the shuttling between the inactivated and conductive states of K^+ channels is accompanied by changes in local outer vestibule dynamics, in the absence of large conformational changes. The altered structural and hydration dynamics of the outer vestibule appear to be likely and important modulators of selectivity filter gating transitions in K^+ channels.

Author contributions: H.R. and E.P. designed research; H.R. performed research; H.R. and S.M. performed fluorescence measurements; S.M.I. and B.R. contributed new reagents/analytic tools; H.R., S.M.I., S.M., B.R., and E.P. analyzed data; and H.R. and E.P. wrote the paper.

The authors declare no conflict of interest.

This article is a PNAS Direct Submission.

[1]To whom correspondence should be addressed. E-mail: eperozo@uchicago.edu.

This article contains supporting information online at www.pnas.org/lookup/suppl/doi:10.1073/pnas.1314875111/-/DCSupplemental.

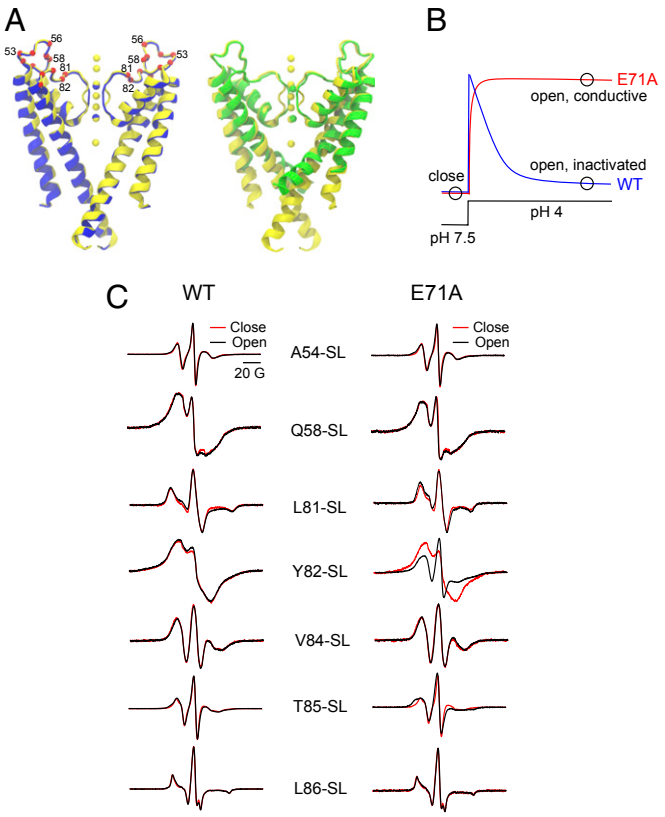

Fig. 1. Comparison of outer vestibule conformation in KcsA structures with conductive and collapsed/inactivated filters. (*A*) High-K^+ KcsA structure [Protein Data Bank (PDB) ID code 1K4C; yellow] is compared with a low-K^+ KcsA structure (PDB ID code 1K4D; blue) in the closed state (*Left*) and open/inactivated conformation (PDB ID code 3F5W; green) (*Right*). The outer vestibule residues are depicted as red spheres, and relevant residues are labeled. (*B*) Schematic representation of typical macroscopic currents elicited by pH-jump experiments in WT (inactivating) and E71A (noninactivating) KcsA channels at a depolarizing membrane potential is shown. Conditions that stabilize the closed, open/inactivated, and open/conductive conformations at the steady state are indicated with a black circle. (*C*) Effect of opening the lower gate on the mobility of spin-labeled outer vestibule residues in palmitoyloleoylphosphatidyl choline/palmitoyloleoylphosphatidyl glycerol (POPC/POPG) (3:1, moles/moles) reconstituted WT (*Left*) and noninactivating mutant E71A (*Right*) backgrounds for the closed (pH 7, red) and open (pH 4, black) states of KcsA, as determined by continuous wave (CW) EPR. The spectra shown are amplitude-normalized. Details are provided in *SI Materials and Methods*.

Results

Changes in Outer Vestibule Conformational Dynamics. Cysteine mutants corresponding to KcsA outer vestibule residues were generated at positions 51–60 and 81–86 in either WT (inactivating) or E71A (noninactivating) background. Of these, residues 51, 53, 55, 59, and 83 did not express well or were not biochemically stable, and therefore were not investigated. Fig. 1*C* shows the gating-induced changes in EPR spectra of spin-labeled mutants of WT and E71A KcsA reconstituted in membranes. As expected from the small structural differences seen in the crystal structures (5, 19) (Fig. 1*A*), there was little or no change in the overall EPR spectral line shape (Fig. 1*C*, *Left*), suggesting the outer vestibule is structurally stable upon inner gate opening and subsequent inactivation. However, when inactivation is abrogated via the E71A mutation, an increase in overall spectral mobility can be seen in a few positions. In particular, the noninactivating Y82-SL/E71A construct shows a considerable reduction in spin-spin coupling (moving away from the permeation path) and a large increase in probe mobility (Fig. 1*C*, *Right*). A direct interpretation of this result would suggest the existence of regions of high dynamics in the outer vestibule as the channel populates the conductive state (18). However, the fact that these changes are not fully reversible (Fig. S1) might suggest additional local effects. In general, EPR is sensitive to nanosecond-to-microsecond time scale motions, whereas fluorescence polarization is sensitive to picosecond-to-nanosecond motions (20). Because the individual subunit chain that forms the outer vestibule in KcsA is in an unusually extended conformation, it is possible that some of the changes in local dynamics are not properly monitored in the EPR time scale. We therefore focused on site-directed fluorescence approaches using the environment-sensitive fluorophore NBD (7-nitrobenz-2-oxa-1,3-diazol-4-yl) (21) to investigate the nature of the outer vestibule dynamics in open/inactivated and open/conductive KcsA further.

Fig. 2 shows the steady-state polarization of KcsA NBD analogs, and its overall changes, under conditions that promote either the inactivated (WT) or conductive (E71A mutant) of the selectivity filter. The polarization values generally indicate that the NBD rotational mobility is representative of motionally restricted environments in the outer vestibule of closed KcsA. However, triggering the opening of the inner bundle gate generates a series of changes in outer vestibule dynamics depending on whether the selectivity filter populates the conductive or the inactivated conformation. In open/inactivated KcsA (WT, low pH), the polarization values are significantly higher for most of the residues (Gly53, Ala54, Gln58, Leu81, and Val84) than for those in the closed state, indicating that the residues in the outer vestibule are more motionally restricted once inactivated (Fig. 2, *Left*). When the same experiment is repeated on the noninactivating E71A KcsA background, some of the outer vestibule residues undergo increased rotational motion (Arg52 and Gly53 in the outer loop and Leu81, Tyr82, and Leu86 in the inner loop above the selectivity filter), reflecting an increased conformational flexibility in the open/conductive conformation. It should be noted that we do not find significant differences in the polarization values in the closed states of WT and E71A KcsA for most of the outer vestibule residues (Fig. S2). However, significant differences in the polarization values do arise upon opening the lower gate of the channel.

Mapping the differences in polarization between the inactivated and conductive conformations illustrates the differential dynamics in the outer vestibule of KcsA during selectivity filter gating (Fig. 2, *Bottom*). Both EPR (Fig. 1*C*, *Right*) and fluorescence polarization experiments demonstrate that the mobility of Tyr82 is similar during inactivation gating but is significantly increased in Y82-SL/E71A and Y82-NBD/E71A constructs. These differential dynamics might be responsible for our recent observation (16) that Cd^{2+} bridges promote the rate of inactivation of Y82C KcsA but have no effect on the noninactivating E71A background. The gating-induced changes in dynamics observed for the E71A/Y82-NBD construct are fully reversible, with macroscopic currents characteristic of E71A KcsA (Fig. S1). These results could be attributed to the perturbed hydrogen bond network between the pore helix and the selectivity filter, and we propose that the higher dynamics of the outer vestibule are a characteristic feature of the open/conductive conformation of K^+ channels.

Changes in Hydration Dynamics During Gating. REES represents a unique and powerful approach that can be used to directly monitor the environment-induced restriction and dynamics around a fluorophore in a complex biological system (see refs. 22 and 23 for reviews and *SI Materials and Methods* for details). Because REES provides information on the relative rates of water relaxation dynamics (24, 25), it is sensitive to changes in local hydration dynamics.

Fig. 3 shows the magnitude of REES for NBD-labeled mutants in both closed and open states under steady-state conditions, along with ΔREES (closed open) mapped in structures, for WT and E71A KcsA. In general, the outer vestibule of KcsA exhibits significant REES, an indication of a motionally restricted

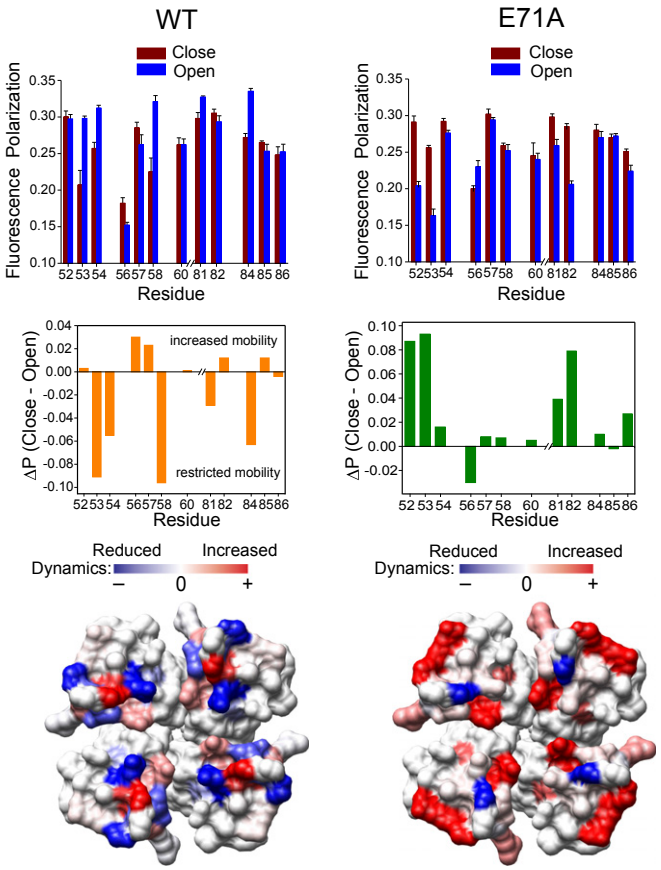

Fig. 2. Outer vestibule of the open/noninactivating conformation is highly dynamic. (*Top*) Steady-state polarization of NBD fluorescence measured for NBD-labeled outer vestibule residues of full-length WT (*Left*) and E71A (*Right*) KcsA reconstituted in POPC/POPG (3:1, moles/moles) liposomes. Measurements at pH 7.5 and pH 4 correspond to the closed and open states of the channel, respectively. The excitation wavelength used was 480 nm; emission was monitored at 535 nm in all cases. The difference in polarization values (ΔP) represent mean ± SE of three independent measurements. The ΔPs (*Middle*) are shown and were mapped on the crystal structure of KcsA (1K4C) to highlight the changes in dynamics between the different functional states of KcsA (*Bottom*) upon gating. Details are provided in *SI Materials and Methods*.

environment. Furthermore, the magnitude of REES (0–6 nm) suggests that there is a considerable difference in the relaxation of solvent molecules (dynamics of hydration) in different positions of the outer vestibule of KcsA. It has been shown that a change of a few nanometers in REES is significant, and the observed changes in the magnitude of REES (0–6 nm) in our case fall within the range of expected REES changes (~5 nm) associated with changes from fully restricted to freely relaxing environments (24, 25). It should be mentioned that REES does not generally provide a quantitative estimate of the water relaxation dynamics because the magnitude of REES is not always linear and is dependent on the given system under investigation (22). In WT KcsA, the solvent relaxation rate is considerably slower around most of the residues during inactivation gating (residues Arg52, Gly53, Ala54, Gln58, and Ile60 in the outer loop and Leu81, Tyr82, and Val84 in the inner loop). This suggests that in the outer vestibule of KcsA, the dynamics of hydration become slower during inactivation gating. In contrast, solvent relaxation is considerably faster in the outer vestibule of channels that remain conductive and do not undergo inactivation (Fig. 3, *Right*). It is interesting to note that these gating-related changes in hydration dynamics are not solely due to changes in the polarity of the local microenvironment, because the outer vestibule residues experience a relatively nonpolar environment in both these states upon gating (Fig. S3). Mapping of ΔREES highlights the changes in hydration dynamics between the open/inactivated and open/conductive outer vestibules of KcsA. Residues surrounding the central pore offer a considerable motional restriction to solvent relaxation dynamics during inactivation gating. These results clearly show that not only is the outer vestibule of open, conductive conformation highly dynamic (Fig. 2) but that the microenvironment associated with the outer vestibule displays faster relaxation. In addition, these results imply a role of bound (restricted) water molecules in inactivation gating (26), and the bound/restricted water could possibly stabilize the inactivated filter long enough to affect K^+ ion permeation (26, 27).

Conformational Changes at the Outer Vestibule of KcsA. The results of the mobility and hydration dynamics suggest that the outer vestibule of KcsA displays different dynamic behavior in the open/inactivated and open/conductive states. This is in agreement with recently reported metal ion binding experiments (16). To probe the changes in structural dynamics further, we measured distances between the symmetrical diagonal subunits of KcsA under conditions that stabilize the conductive and inactivated filter conformations. Using tandem dimer (TD) constructs (28), long distances (~>20 Å) were measured using double electron-electron resonance (DEER) spectroscopy (29), whereas short distances (~<20 Å) were monitored using continuous wave EPR dipolar broadening experiments.

Outer vestibule distances and distance histograms from inactivating (WT) and noninactivating (E71A) KcsA are shown in Figs. S4 and S5. The analysis of conformational changes in the outer vestibule in different functional states of KcsA is complicated due to broad and heterogeneous distance distributions. Nevertheless, mapping the distance differences between closed and open states from the predominant distance peak (Fig. S6) suggests that residues surrounding the central pore tend to come closer to each other in the open/inactivated state, in line with earlier metal ion binding experiments (16). However, this constricting transition does not seem to be present in the open/noninactivating (conductive) conformation (Fig. S6), as reported recently (30).

Although there is a considerable change in intersubunit distances as KcsA transitions between the inactivated and conductive conformations, it is difficult to interpret these changes at the backbone level due to broad and heterogeneous distance distributions. We have used a recently developed molecular dynamics simulation technique, the RE method (31, 32), to evaluate the degree of overall motion in the outer vestibule using the experimentally derived distance histograms (Figs. S7 and S8) obtained from DEER distance determinations. In the RE method, interspin distance distribution histograms calculated from multiple spin label copies in a molecular dynamics simulation are forced to match those obtained from experimentally derived distance histograms via a global ensemble-based energy restraint. The closed/conductive [Protein Data Bank (PDB) ID code 1K4C], open/inactivated (PDB ID code 3F5W), and "flipped" E71A (PDB ID code 2ATK) conformations of KcsA were used as templates in all RE simulations. A representative KcsA structure with multiple copies of spin labels attached to positions 57 and 86 in the outer vestibule is shown in Fig. 4*A*. The final models for the outer vestibule, obtained using the RE method and several refinement cycles, for all three structures of KcsA are shown in Fig. 4*B*, along with the respective changes in rmsd (for residues 51–88) as a function of refinement cycles (Fig. 4*C*). Our calculations suggest that there are no major static conformational changes in the outer vestibule of different functional states of KcsA compared with the starting template structures (Fig. 4*B*). The change in rmsd for the backbone atoms is modest and is in the range of ~0.4–1.0 Å (Fig. 4*C* and Table S1). It is interesting to note that even for the flipped E71A starting structure, which differs significantly from other starting conformations, changes in rmsd do not exceed ~1 Å. These results suggest that all structures are physiologically relevant and the modest conformational

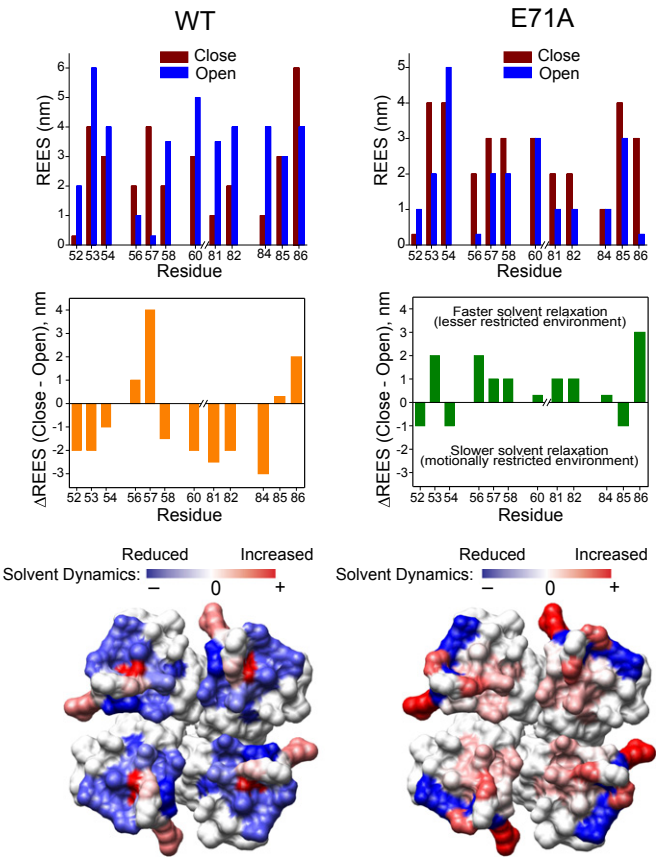

Fig. 3. Solvent relaxation dynamics probed by the REES. REES of NBD-labeled outer vestibule residues of full-length WT (*Left*) and E71A (*Right*) KcsA reconstituted in POPC/POPG (3:1, moles/moles) liposomes. Measurements at pH 7.5 and pH 4 correspond to the closed and open states of the channel. (*Top*) Change in the emission maximum (in nanometers) as a function of changing the excitation wavelength from 465 to 515 nm is shown as the REES. The error is typically ±0.5 nm of the reported values. The difference in REES values (ΔREES) (*Middle*) are shown and were mapped on the crystal structure of KcsA to highlight the changes in solvent relaxation dynamics between different functional states of KcsA (*Bottom*) upon gating. Details are provided in *SI Materials and Methods*.

change in the outer vestibule seen in several crystal structures of KcsA might not be a Fab-mediated conformation. Further, this clearly suggests that the side-chain conformational dynamics at the KcsA outer vestibule might be responsible for the functional differences observed during inactivation and noninactivation gating (12, 16).

Discussion

There is now ample evidence suggesting that in K^+ channels, the selectivity filter and its support structures (the pore helix and the outer vestibule) play a key role in gating, both at the slow (C-type inactivation) and fast (single-channel flicker) time scales (3, 5, 12, 13, 15, 16, 18, 19, 33–36). Indeed, strong experimental evidence points to the hydrogen bond network behind the selectivity filter as a driver of the inactivation process (12, 13, 15).

The outer vestibule of KcsA is an important unstructured region in which toxins (37), blockers (35, 38), and metal ions (16) bind and modulate the gating behavior of K^+ channels. Several results suggest a dynamic structural rearrangement in the outer vestibule during C-type inactivation gating in KcsA and *Shaker* K^+ channels (16, 18, 19). However, despite its functional importance, the outer vestibule does not show appreciable conformational changes in several crystal structures of KcsA trapped in various functional states (5, 17). Because the high-resolution KcsA crystal structures were obtained using Fab that binds at the outer mouth of the pore and slows down the rate of inactivation (12), it is reasonable to speculate that Fab binding limits the functionally relevant conformational changes. We have looked into this issue by monitoring the structural dynamics of the outer vestibule in KcsA under conditions that stabilize different functional conformations.

Our results show that the conformational dynamics of the outer vestibule change according to the functional state of the channel. During inactivation gating, the mobility of the outer vestibule is restricted, whereas the outer vestibule is highly dynamic in the open/conductive conformation of KcsA (Fig. 2). This is consistent with earlier findings on the *Shaker* K^+ channel, which indicate that the C-type–inactivated state is more ordered than the noninactivated state (39). In particular, the spectroscopic probes (nitroxide spin label and NBD fluorophore) attached to Y82C KcsA show a significant increase in dynamics as the lower gate opens and the selectivity filter remains in the conductive conformation (E71A mutant). Further, unlike in the inactivated conformation (16), the average distance obtained between spin labels in the TD Y82C KcsA changes from 12 Å in the closed state to ∼17 Å in the noninactivating E71A mutant, indicating that the selectivity filter appears to be more plastic in the open/conductive conformation (Fig. S5). This is supportive of the alternate conformations of the Y82 side chain in the outer vestibule, as seen in the flipped structure of E71A (12). In the crystal structures of WT KcsA and flipped E71A KcsA, the difference in the distance between the C_α-C_α and OH-OH atoms of Tyr82 residues in diagonally symmetrical subunits increases by ∼0.8 Å and ∼4.3 Å, respectively. The excursion between two orientations of the Tyr82 side chain might therefore be responsible for the ∼50-fold lower extracellular TEA affinity observed in E71A KcsA (38) and for the inability of cadmium ions

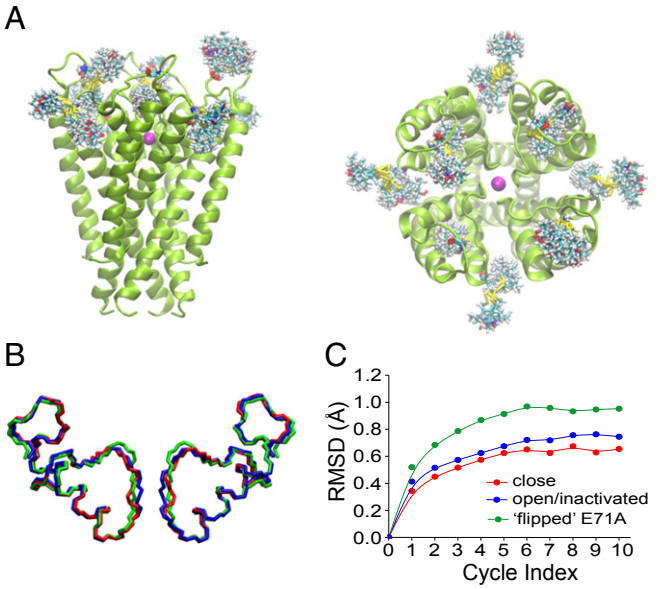

Fig. 4. "All-atom" RE simulations. (*A*) Side view (*Left*) and top view (*Right*) of the WT KcsA tetramer (PDB ID code 1K4C) with multiple copies of the spin label (shown as sticks) attached in silico to positions 57 and 86. The potassium ion (K^+) is shown as magenta spheres. (*B*) Backbone conformations corresponding to residues 51–88 representative of closed (red), open/inactivated (blue), and conductive (flipped E71A, green) conformations derived after RE simulations using the respective experimentally derived histograms for the closed, open/inactivated, and open/conductive states of KcsA. (*C*) Change in rmsd as a function of refinement cycle index during RE simulations for closed (red), open/inactivated (blue), and conductive (flipped E71A, green) states of KcsA with respect to the template structures used. Details are provided in *SI Materials and Methods*.

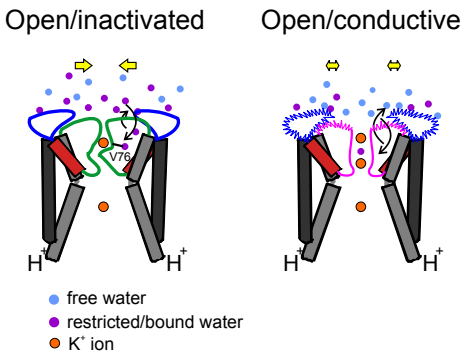

Fig. 5. Gating-induced structural dynamics at the outer vestibule of KcsA. Schematic representations of the events associated with the outer vestibule in open/inactivated (*Left*) and open/conductive (*Right*) conformations of KcsA are shown. The diagonally symmetrical subunits are shown for clarity. (*Right*) Outer vestibule is highly dynamic in open/conductive conformations, as depicted by the wiggly nature of the outer vestibule. Further, upon gating, the hydration dynamics are faster in the open/conductive conformation, which is indicative of the increased ratio of bulk/free (blue spheres) vs. restricted/bound (purple spheres) water molecules. (*Left*) In contrast, the opening of the activation gate imposes motional restriction on the outer vestibule in channels that undergo inactivation. This is accompanied by increased restricted/bound water molecules that might play an important role in further stabilizing the inactivated/collapsed (26, 27) filter by possibly interacting with selectivity filter residues (V76 is shown as an example). The exchange rate of water molecules in the selectivity filter and the outer vestibule is shown as curved arrows. (*Left*) Tendency of the side chains to come closer during inactivation gating is depicted as yellow arrows. Details are provided in *Discussion*.

to form metal bridges between adjacent subunits in the open/conductive conformation of Y82C KcsA (16). Based on these results, it is tempting to suggest that the Y82 side-chain conformation observed in the flipped E71A structure, possibly due to increased outer vestibule dynamics, could be a characteristic feature in the open/conductive conformation of KcsA, especially when the strength of the interaction between the pore helix and the outer mouth is disrupted.

Hydration and dynamics play an important role in lipid–protein interactions (21) and ion channel selectivity (40) because protein fluctuations, slow solvation, and the dynamics of hydrating water are all intrinsically related (41). It has been shown that heterogeneity in the dynamics of water interactions is coupled to differential time scales of hydrogen bond formation and breaking (42). Using a wavelength-selective fluorescence approach (REES), we showed that entry to the inactivated state is associated with the presence of restricted/bound water molecules in the outer vestibule of KcsA (Fig. 3). These restricted/bound water molecules might potentially act as hydrogen bonding ligands with the residues associated with the selectivity filter, affecting filter dynamics and kinetics of entry and exit from the inactivated state (26, 27).

It is interesting to note that three crystallographic water molecules are present in the nonconducting filter conformation (1K4D) behind the selectivity filter, whereas only one buried ordered water molecule is observed in the crystal structure of the conductive filter (1K4C). Very recently, using a long molecular dynamics simulation (~17 μs), it has been shown that the recovery from C-type inactivation is directly controlled by these buried ordered water molecules (26), thus making these restricted/bound water molecules a vital part of the protein structure when the selectivity filter is trapped in the nonconductive conformation. Additional evidence of the presence of bound water molecules comes from a recent NMR study (27), which shows that the carbonyl group of V76 seems to form hydrogen bonds with the water molecule in the selectivity filter only in the inactivated state. In contrast, we observed a relatively fast solvent relaxation in the open/conductive state, suggesting that the water molecules in the outer vestibule and behind the selectivity filter might be rapidly exchanging with free/bulk water. These increased dynamics of hydration are consistent with the dynamic properties of the open/conductive outer vestibule, as seen in the E71A mutant (Fig. 2). The nature of differential hydration dynamics in the outer vestibule of different functional states of KcsA support a role for water molecules in selectivity filter gating of K^+ channels, and could be relevant in understanding the interplay between ions, the selectivity filter, and the resulting distinct gating fluctuations (26, 36, 43).

RE simulations, along with distance measurements, support modest backbone conformational changes in the outer vestibule of KcsA in the open/conductive and open/inactivated states. This reiterates the role of side-chain conformational dynamics in modulating the gating mechanisms in K^+ channels. Importantly, such conformational changes in the side chains of several key residues, such as Trp67, Asp80, and Tyr82, are observed in the flipped E71A structure (12). The outward "flipping" of the Asp80 side chain relative to its position in WT KcsA has been observed in flipped E71A [both high K^+ (12) and low K^+ (33)] and other Glu71 mutants that exhibit substantial loss of C-type inactivation (36), as well as in the Kir 3.1 channel (44).

We propose a model (Fig. 5) that shows key differences associated with the outer vestibule in open/inactivated and open/conductive conformations of KcsA and their likely consequences in gating mechanisms. The outer vestibule is highly dynamic in channels that do not undergo inactivation, which is accompanied by increased hydration dynamics. In contrast, the outer vestibule of the inactivated state is motionally restricted, and the restricted/bound water molecules might play a crucial role in modulating the extent of inactivation. This might involve binding of water molecules to selectivity filter residues in the inactivated state, most notably the carbonyl group of V76 when it flips away from the conduction pathway (5, 26, 27, 36). Depending on the relative water relaxation dynamics, the exchange between the bound and free water might therefore be affected, which, in turn, would affect the organization and occupancy of water molecule(s) behind the selectivity filter. The conformational change of the outer vestibule, on average, is modest when the channel transits between different functional states, and the constriction of the pore is possible only in the inactivated state depending on the presence of external ligands, such as metal ions (16). In the open/conductive conformation, the concerted changes due to increased dynamics and flipping of Asp80 and Tyr82 might not allow the outer mouth to constrict the pore, thereby eliminating inactivation by preventing the selectivity filter from collapsing. Overall, this model highlights the importance of the hydrogen bond network behind the selectivity filter, side-chain conformational dynamics, and microscopic observables (e.g., water molecules) in the gating mechanisms of K^+ channels.

Materials and Methods

We have used pQE32-KcsA construct in all cases. Tandem dimer constructs of KcsA were used for distance measurements. Detailed information regarding cloning, mutagenesis, channel biochemistry, generation of tandem KcsA constructs, liposome patch-clamp, fluorescence and EPR spectroscopy, and DEER and RE simulations can be found in *SI Materials and Methods*.

ACKNOWLEDGMENTS. We thank F. Bezanilla (The University of Chicago) for providing access to the Photon Technology Instruments steady-state spectrofluorometer. This work was supported in part by National Institutes of Health Grant R01-GM57846 (to E.P.).

1. Yellen G (1998) The moving parts of voltage-gated ion channels. *Q Rev Biophys* 31(3):239–295.
2. Perozo E, Cortes DM, Cuello LG (1999) Structural rearrangements underlying K^+-channel activation gating. *Science* 285(5424):73–78.
3. Kurata HT, Fedida D (2006) A structural interpretation of voltage-gated potassium channel inactivation. *Prog Biophys Mol Biol* 92(2):185–208.
4. Long SB, Campbell EB, Mackinnon R (2005) Crystal structure of a mammalian voltage-dependent Shaker family K^+ channel. *Science* 309(5736):897–903.

5. Cuello LG, Jogini V, Cortes DM, Perozo E (2010) Structural mechanism of C-type inactivation in K(+) channels. *Nature* 466(7303):203–208.
6. Cuello LG, et al. (2010) Structural basis for the coupling between activation and inactivation gates in K(+) channels. *Nature* 466(7303):272–275.
7. Hoshi T, Zagotta WN, Aldrich RW (1991) Two types of inactivation in *Shaker* K+ channels: Effects of alterations in the carboxy-terminal region. *Neuron* 7(4):547–556.
8. Bean BP (2007) The action potential in mammalian central neurons. *Nat Rev Neurosci* 8(6):451–465.
9. Baukrowitz T, Yellen G (1995) Modulation of K+ current by frequency and external [K^+]: A tale of two inactivation mechanisms. *Neuron* 15(4):951–960.
10. López-Barneo J, Hoshi T, Heinemann SH, Aldrich RW (1993) Effects of external cations and mutations in the pore region on C-type inactivation of Shaker potassium channels. *Receptors Channels* 1(1):61–71.
11. Choi KL, Aldrich RW, Yellen G (1991) Tetraethylammonium blockade distinguishes two inactivation mechanisms in voltage-activated K^+ channels. *Proc Natl Acad Sci USA* 88(12):5092–5095.
12. Cordero-Morales JF, et al. (2006) Molecular determinants of gating at the potassium-channel selectivity filter. *Nat Struct Mol Biol* 13(4):311–318.
13. Cordero-Morales JF, et al. (2007) Molecular driving forces determining potassium channel slow inactivation. *Nat Struct Mol Biol* 14(11):1062–1069.
14. Gao L, Mi X, Paajanen V, Wang K, Fan Z (2005) Activation-coupled inactivation in the bacterial potassium channel KcsA. *Proc Natl Acad Sci USA* 102(49):17630–17635.
15. Cordero-Morales JF, Jogini V, Chakrapani S, Perozo E (2011) A multipoint hydrogen-bond network underlying KcsA C-type inactivation. *Biophys J* 100(10):2387–2393.
16. Raghuraman H, et al. (2012) Mechanism of Cd^{2+} coordination during slow inactivation in potassium channels. *Structure* 20(8):1332–1342.
17. Zhou Y, Morais-Cabral JH, Kaufman A, MacKinnon R (2001) Chemistry of ion coordination and hydration revealed by a K+ channel-Fab complex at 2.0 A resolution. *Nature* 414(6859):43–48.
18. Yellen G, Sodickson D, Chen T-Y, Jurman ME (1994) An engineered cysteine in the external mouth of a K+ channel allows inactivation to be modulated by metal binding. *Biophys J* 66(4):1068–1075.
19. Liu Y, Jurman ME, Yellen G (1996) Dynamic rearrangement of the outer mouth of a K^+ channel during gating. *Neuron* 16(4):859–867.
20. Thomas DD (1978) Large-scale rotational motions of proteins detected by electron paramagnetic resonance and fluorescence. *Biophys J* 24(2):439–462.
21. Raghuraman H, Chattopadhyay A (2007) Orientation and dynamics of melittin in membranes of varying composition utilizing NBD fluorescence. *Biophys J* 92(4): 1271–1283.
22. Raghuraman H, Kelkar DA, Chattopadhyay A (2005) Novel insights into protein structure and dynamics utilizing the red edge excitation shift. *Reviews in Fluorescence 2005*, eds Geddes CD, Lakowicz JR (Springer, New York), pp 199–222.
23. Demchenko AP (2008) Site-selective Red-Edge effects. *Methods Enzymol* 450:59–78.
24. Chattopadhyay A, Mukherjee S, Raghuraman H (2002) Reverse micellar organization and dynamics: A wavelength-selective fluorescence approach. *J Phys Chem B* 106(50): 13002–13009.
25. Raghuraman H, Chattopadhyay A (2003) Organization and dynamics of melittin in environments of graded hydration. *Langmuir* 19(24):10332–10341.
26. Ostmeyer J, Chakrapani S, Pan AC, Perozo E, Roux B (2013) Recovery from slow inactivation in K^+ channels is controlled by water molecules. *Nature* 501(7465):121–124.
27. Imai S, Osawa M, Takeuchi K, Shimada I (2010) Structural basis underlying the dual gate properties of KcsA. *Proc Natl Acad Sci USA* 107(14):6216–6221.
28. Liu Y-S, Sompornpisut P, Perozo E (2001) Structure of the KcsA channel intracellular gate in the open state. *Nat Struct Biol* 8(10):883–887.
29. Jeschke G (2012) DEER distance measurements on proteins. *Annu Rev Phys Chem* 63: 419–446.
30. Bhate MP, McDermott AE (2012) Protonation state of E71 in KcsA and its role for channel collapse and inactivation. *Proc Natl Acad Sci USA* 109(38):15265–15270.
31. Roux B, Islam SM (2013) Restrained-ensemble molecular dynamics simulations based on distance histograms from double electron-electron resonance spectroscopy. *J Phys Chem B* 117(17):4733–4739.
32. Islam SM, Stein RA, McHaourab HS, Roux B (2013) Structural refinement from restrained-ensemble simulations based on EPR/DEER data: Application to T4 lysozyme. *J Phys Chem B* 117(17):4740–4754.
33. Cheng WWL, McCoy JG, Thompson AN, Nichols CG, Nimigean CM (2011) Mechanism for selectivity-inactivation coupling in KcsA potassium channels. *Proc Natl Acad Sci USA* 108(13):5272–5277.
34. Claydon TW, Makary SY, Dibb KM, Boyett MR (2003) The selectivity filter may act as the agonist-activated gate in the G protein-activated Kir3.1/Kir3.4 K^+ channel. *J Biol Chem* 278(50):50654–50663.
35. Ader C, et al. (2008) A structural link between inactivation and block of a K^+ channel. *Nat Struct Mol Biol* 15(6):605–612.
36. Chakrapani S, et al. (2011) On the structural basis of modal gating behavior in K(+) channels. *Nat Struct Mol Biol* 18(1):67–74.
37. Zachariae U, et al. (2008) The molecular mechanism of toxin-induced conformational changes in a potassium channel: Relation to C-type inactivation. *Structure* 16(5): 747–754.
38. Vales E, Raja M (2010) The "flipped" state in E71A-K^+-channel KcsA exclusively alters the channel gating properties by tetraethylammonium and phosphatidylglycerol. *J Membr Biol* 234(1):1–11.
39. Meyer R, Heinemann SH (1997) Temperature and pressure dependence of Shaker K+ channel N- and C-type inactivation. *Eur Biophys J* 26(6):433–445.
40. Noskov SY, Roux B (2007) Importance of hydration and dynamics on the selectivity of the KcsA and NaK channels. *J Gen Physiol* 129(2):135–143.
41. Li T, Hassanali AA, Kao YT, Zhong D, Singer SJ (2007) Hydration dynamics and time scales of coupled water-protein fluctuations. *J Am Chem Soc* 129(11):3376–3382.
42. Jana M, Bandyopadhyay S (2012) Restricted dynamics of water around a protein-carbohydrate complex: Computer simulation studies. *J Chem Phys* 137(5):055102.
43. Dreyer I, Michard E, Lacombe B, Thibaud JB (2001) A plant Shaker-like K^+ channel switches between two distinct gating modes resulting in either inward-rectifying or "leak" current. *FEBS Lett* 505(2):233–239.
44. Nishida M, Cadene M, Chait BT, MacKinnon R (2007) Crystal structure of a Kir3.1-prokaryotic Kir channel chimera. *EMBO J* 26(17):4005–4015.